Journal of Energy

VOLUME 66 Number 1–4 | 2017 Special Issue

journal homepage: http://journalofenergy.com/

BRUNO JURIŠIĆ bruno.jurisic@fer.hr

LUKA BUČAR luka.bucar@dalekovod.hr

IVO UGLEŠIĆ ivo.uglesic@fer.hr

University of Zagreb Faculty of Electrical Engineering and Computing

CALCULATION OF VOLTAGE DISTRIBUTION ALONG THE TRANSFORMER WINDING USING THE WIDE BAND TRANSFORMER MODEL

SUMMARY

Electrical devices in transmission and distribution networks are submitted to fast front transients. These transients are often a cause of a failure in the power system. To simulate these phenomena, it is necessary to detailly model all the components of the power system. This paper concentrates on studding transformer internal failures due to voltage stress that can occur when fast front electromagnetic wave travels through the transformer. To prevent a failure, an internal insulation of the transformer has to be dimensioned to sustain these transient phenomena. Therefore, it is necessary to use advanced wideband transformer models for its dimensioning.

In this paper, a wide band transformer model based on limited transformer geometry is used to simulate evaluate the stresses on internal transformer insulation in the case of fast front transients. The model is validated for calculation of internal overvoltages with the test case from CIGRE brochure.

Key words: Fast front transients, transformer, Grey Box, internal insulation, voltage distribution.

1. INTRODUCTION

Electrical equipment is designed to work permanently at nominal values of frequency, voltage and current. However, transient phenomena occur in the power system affecting the normal operation of the system and its components. These phenomena can reduce life time of the equipment or cause permanent damage to the equipment which has not been dimensioned and protected properly.

In this paper, a power transformer and its behaviour during fast front transients has been studied. These transients include frequencies from few tens of kHz up to few hundreds of kHz. Such fast electromagnetic wave, that encounters transformer windings, is non-linearly distributed along the transformer winding, causing the stress on the inner insulation of the transformer. Therefore, in the design stage of the transformer as well as during the investigation system studies it is necessary to simulate these voltages correctly. To do so, complex wide band transformer models based on the transformer geometry have to be used [1], [2]. As the detailed geometry data needed for these models is not always available, the model that requires a limited information about the transformer geometry data has been developed recently [3], [4]. To validate it for studding the internal voltages, a model is used for modelling a CIGRE test case transformer and compared with the responses that have been calculated using the detailed transformer models that have been developed by different transformer manufacturers.

In the second section of this paper an electromagnetic behaviour of a power transformer has been described when fast front electromagnetic wave is applied to its terminals. In the third section, a "Grey Box" model used in the study is described. Then, in the fourth the test case geometry for a fictitious 100 MVA, 230/69 kV transformer is presented. It includes a validation based on the comparison with the results that have been calculated using the others, already validated models. Finally, the fifth is a conclusion.

2. ELECTROMAGNETIC BEHAVIOUR OF A TRANSFORMER WHEN SUBJECTED TO A FAST-FRONT ELECTROMAGNETIC WAVE

In this section of the paper an electromagnetic behaviour of a transformer, when it is subjected to the electromagnetic wave caused which contains high frequencies in the range of few tens or hundreds of kHz, is explained.

Fast-front transients in power systems are generally caused by lightning or more rarely by vacuum circuit breaker switching and they usually have an amplitude larger than the ones existing because of any other transients. They are critical for choosing the withstand voltage of the power system equipment. The maximum frequency of these transients ranges between 50 and 10000 kHz while its lowest frequency is less than 3.33 kHz [5]. The standard test voltage shape is 1.2/50 μs lightning impulse test wave, defined in [6].

The response of a transformer submitted to high frequency overvoltages and the corresponding voltage distribution along its windings highly depend on the frequency spectrum of the overvoltages, which are applied to the transformer terminals. Table 1, which is extracted from [7], presents the influence of the main transformer parameters versus the type of transient:

Table 1: Transformer parameters sensitivity versus frequency [7].

Parameter/ Effect	Low-Frequency Transients	Slow-Front Transients	Fast-Front Transients	Very Fast-Front Transients
Short circuit impedance	Very important	Very important	Important	Negligible
Saturation	Very important	Important	Negligible	Negligible
Core losses	Very important	Important	Eddy currents losses are important*	Negligible
Capacitive coupling	Negligible	Important	Very important	Very important

Note that the element from Table 1 marked with an asterisk differs from the one of the table given in [7].

First parameter, shown in Table 1, refers to the leakage inductance and losses in the conductor when a current flows through it (Joules losses and eddy current losses). Eddy currents losses in the windings rise versus frequency as well as the impedance of the leakage flux reactance. Consequently, less current flows through the transformer windings. Therefore, the influence of the short circuit impedance diminishes with frequency. Nevertheless, for fast front transients it is important to model correctly eddy current losses (skin and proximity losses) in the copper of the windings, especially if the model is intended to have an accurate damping.

The two following parameters from Table 1, namely saturation and core losses, are related to the core influence. For fast front and very fast front transients it can be considered that the magnetic flux disappears from the core with high frequencies due to the rise of the eddy currents in the core's lamination which compensate the main flux, resulting in the low magnetic induction in the core. Consequently the core's permeability is considered to be in its initial zone (linear part of the saturation curve) so saturation effect and hysteresis losses can be neglected [8], [9].

The last parameter in Table 1, capacitive coupling between the windings and between the windings and the ground becomes important when modelling a transformer for fast front and very fast front transients.

3. GREY BOX TRANSFORMER MODEL

Following the observations in the previous section, a Grey Box model l on limited information about the transformer geometry has been developed to : high frequency overvoltages existing on outside and inside terminals o transformer [3], [4], [10].

The model is composed of lumped RLCG equivalent parameters whose v are calculated using finite element method software program [11]. In the mode transformer geometry is divided in simple segments as shown in Figure 1.

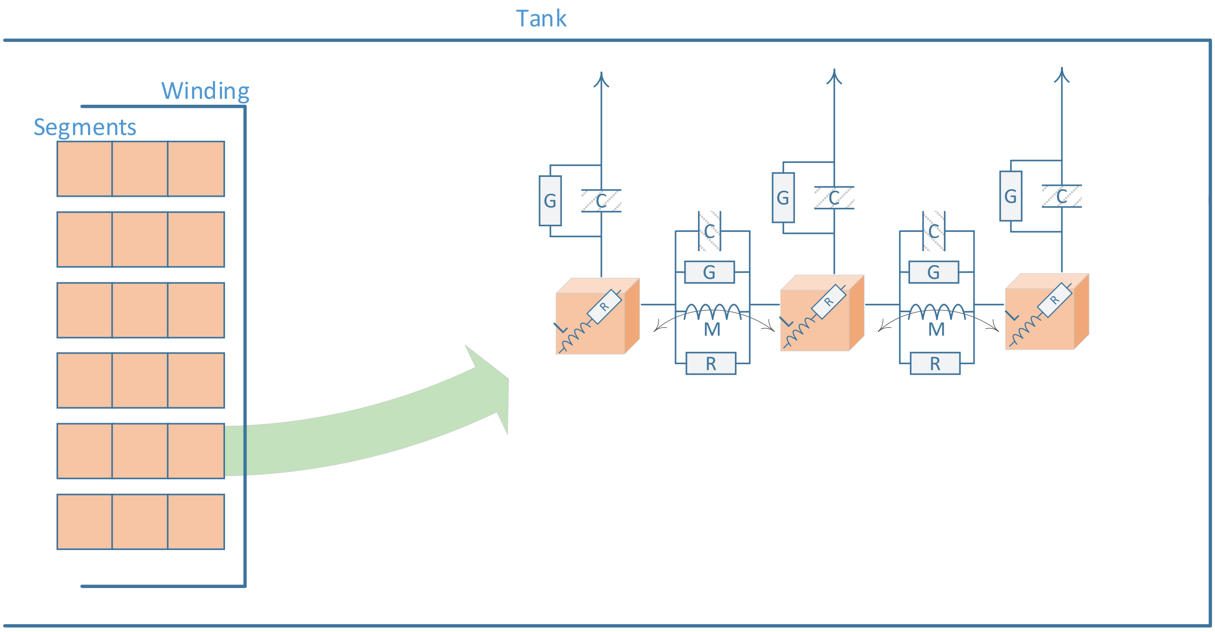

Figure 1: Segment of the Grey Box transformer model

Each segment represents a turn or a group of the turns depending o transformer size and the frequency range that needs to be simulated. S segment consists of serial inductance, serial resistance, serial capacitances, m inductances, capacitances and resistances (related to the proximity effect) capacitances and conductance to the ground. Resistance and inductance param are frequency dependent since eddy current effects (proximity and skin effect represented in the model. This is important to model if one wants to have acc dumping at high frequencies.

Inductances and resistances are calculated from the magnetic field valu given frequency by using the Maxwell Ampere's law for quasistatic magnetic ($\nabla\times\boldsymbol{B}=\mu\boldsymbol{J}$) from which the following equations can be extracted [12]:

$$R_{ij} = -\frac{\omega * n_j}{\mathbf{I_i}} * \operatorname{Im}\left\{\oint_{C_j}\left(\frac{n_i}{a_j}\iint_{S_j}\mathbf{A_{ij}}\,d\mathbf{S_j}\right)d\mathbf{l_j}\right\} \tag{1}$$

$$L_{ij} = \frac{n_j}{\mathbf{I_i}} * \operatorname{Re}\left\{\oint_{C_j}\left(\frac{n_i}{a_j}\iint_{S_j}\mathbf{A_{ij}}\,d\mathbf{S_j}\right)d\mathbf{l_j}\right\} \tag{2}$$

Capacitance values are calculated from the electrostatic electric field calculations, from the charge:

$$C_{ij} = \frac{Q_{ij}}{V_i} \quad (3)$$

Conductance parameters are calculated directly from capacitance parameters [3], [8].

When all the parameters are calculated, it is possible to form branch impedance matrix $\boldsymbol{Z_{RLbranch}}$ and nodal admittance matrix $\boldsymbol{Y_{CGnodal}}$ as follows:

$$\boldsymbol{Z_{RLbranch}}(f) = \boldsymbol{R}(f) + j\omega\boldsymbol{L}(f) \quad (4)$$

$$\boldsymbol{Y_{CGnodal}}(f) = \boldsymbol{G}(f) + j\omega\boldsymbol{C} \quad (5)$$

Both matrices $\boldsymbol{Z_{RLbranch}}(f)$ and $\boldsymbol{Y_{GCnodal}}(f)$ are symmetrical. All the elements of the matrices given above, except the capacitances, are frequency dependant. Dimension of $\boldsymbol{Z_{RLbranch}}(f)$ is determined by the number of segments taken into consideration while the dimension of $\boldsymbol{Y_{GCnodal}}(f)$ is determined by the number of nodes.

To calculate a transformer nodal admittance matrix, first, it is necessary to calculate $\boldsymbol{RL}$ nodal matrix, $\boldsymbol{Y_{RLnodal}}(f)$ from the $\boldsymbol{Z_{RLbranch}}(f)$ matrix:

$$\boldsymbol{Y_{RLnodal}}(f) = \boldsymbol{A} * \boldsymbol{Z_{RLbranch}}(f)^{-1} * \boldsymbol{A}^T \quad (6)$$

$\boldsymbol{A}$ is the incidence matrix which contains the relations between the inductive branch currents and the nodal currents [3]. The $\boldsymbol{Y_{RLnodal}}(f)$ matrix is a square matrix of the dimension equal to the number of nodes.

Complete nodal matrix of a transformer, $\boldsymbol{Y_{nodal}}(f)$ can be calculated as follows:

$$\boldsymbol{Y_{nodal}}(f) = \boldsymbol{Y_{RLnodal}}(f) * \boldsymbol{Y_{RLnodal}}(f) \quad (7)$$

$$\boldsymbol{Y_{nodal}}(f) = \begin{bmatrix} \boldsymbol{Y_{ee}}(f) & \boldsymbol{Y_{ei}}(f) \\ \boldsymbol{Y_{ie}}(f) & \boldsymbol{Y_{ii}}(f) \end{bmatrix} \quad (8)$$

$$\begin{bmatrix} \boldsymbol{Y_{ee}}(f) & \boldsymbol{Y_{ei}}(f) \\ \boldsymbol{Y_{ie}}(f) & \boldsymbol{Y_{ii}}(f) \end{bmatrix} * \begin{bmatrix} \boldsymbol{V_e}(f) \\ \boldsymbol{V_i}(f) \end{bmatrix} = \begin{bmatrix} \boldsymbol{I_e}(f) \\ \boldsymbol{I_i}(f) \end{bmatrix} \quad (9)$$

$\boldsymbol{V_e}$ and $\boldsymbol{I_e}$ respectively stand for the voltages at the external terminals and currents flowing into the external terminals while $\boldsymbol{V_i}$ and $\boldsymbol{I_i}$ stand for the voltages at the internal terminals and currents flowing into the internal terminals. To form a nodal matrix as it is shown in equation (8) the rows and columns of the nodal matrix have to be restacked.

If in equation (9) we set all the currents that are entering in internal transformer nodes, $\boldsymbol{I_i}$ to 0, then it can be written:

$$\boldsymbol{V_i}(f) = -\boldsymbol{V_{ii}}(f)^{-1} * \boldsymbol{V_{ie}}(f) * \boldsymbol{V_e}(f) \tag{10}$$

As the vector of external voltages, $\boldsymbol{V_e}$ (which is calculated using the EMTP type software progrann) is in the time domain, Fast Fourier Transform has to be used to transform it to the frequency domain. Once the external voltages are transformed in the frequency domain, equation (10) can be applied. To show the internal voltages, $\boldsymbol{V_i}$ in the time domain, Inverse Fast Fourier Transform has to be used.

4. TEST CASE SCENARIO

In this section a fictitious two windings 100 MVA, 230/69 kV transformer is presented and validated for a given test scenario. The comparison between the presented model results and other, already validated models has been shown [1].

As a fictitious transformer model, the technical advances used to produce the transformer are exempted from the transformer's design so it isn't optimal. For instance, the conductors used for windings are larger than the standard ones and the insulation is oversized.

Transformer consists of one low voltage winding and one high voltage winding (which has two segments connected in parallel) mounted around central leg of three-legged core. Coordinates of the winding and core's geometry are shown in Figure 2.

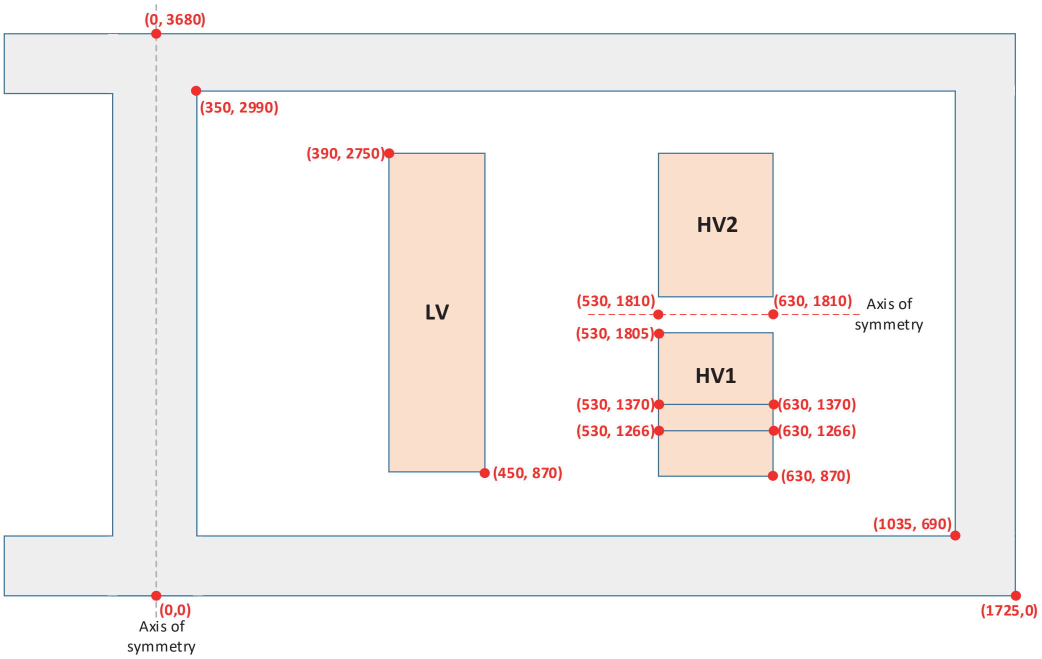

Figure 2: Transformer window and winding coordinates for model plotting (mm)

Both windings are discs windings. The low voltage winding is modelled with 87 discs and 5 turn per discs while the high voltage winding is modelled with 84 discs per part of the winding and 20 turns per discs. The high voltage winding is interleaved. For more details on the transformer geometry, see [1].

For the simplicity, in the paper only one test scenario is described. It is assumed that 1050 kV lightning impulse wave hits HV terminal of high voltage winding, while all the other terminals are grounded. This scenario is similar to lightning impulse test that is a routine test for all the transformer with nominal voltage higher than 72.5 kV [13].

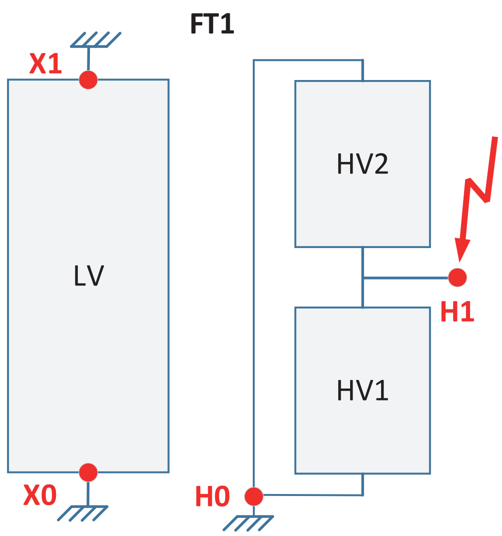

Figure 3: Test scenario

The transformer is modelled using the described Grey Box model, representing 5 turns as one segment. This approximation reduced number of the elements in the model from 2115 to 423. The accuracy of the model is maintained up to 780 kHz. As two parts of the HV winding are connected in parallel, the model is constructed in the way that the voltage distributions do not differ for two parallels. This has been done in order to reduce the simulation time. Therefore, the results are shown only for one parallel HV branch (see nodes from 45 to 68 in Figure 4). Associated numbers with the LV winding are 1 to 44. External nodes are named as follows: "LV1", "LV_mid", "H0" and "H1".

In the continuation the results are compared with the one provided in CIGRE brochure [1] for the maximum voltage amplitude that exist in all the internal nodes when LI is applied to terminal H1.

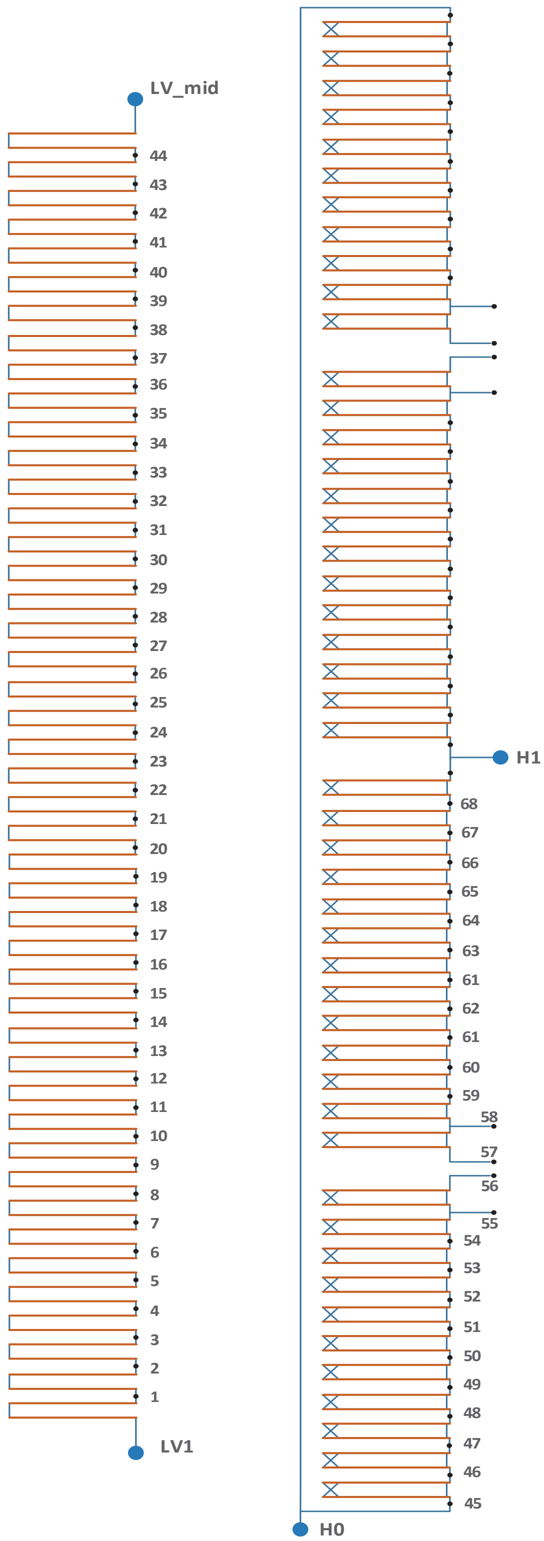

Figure 4: Names of internal and external nodes in LV and HV windings

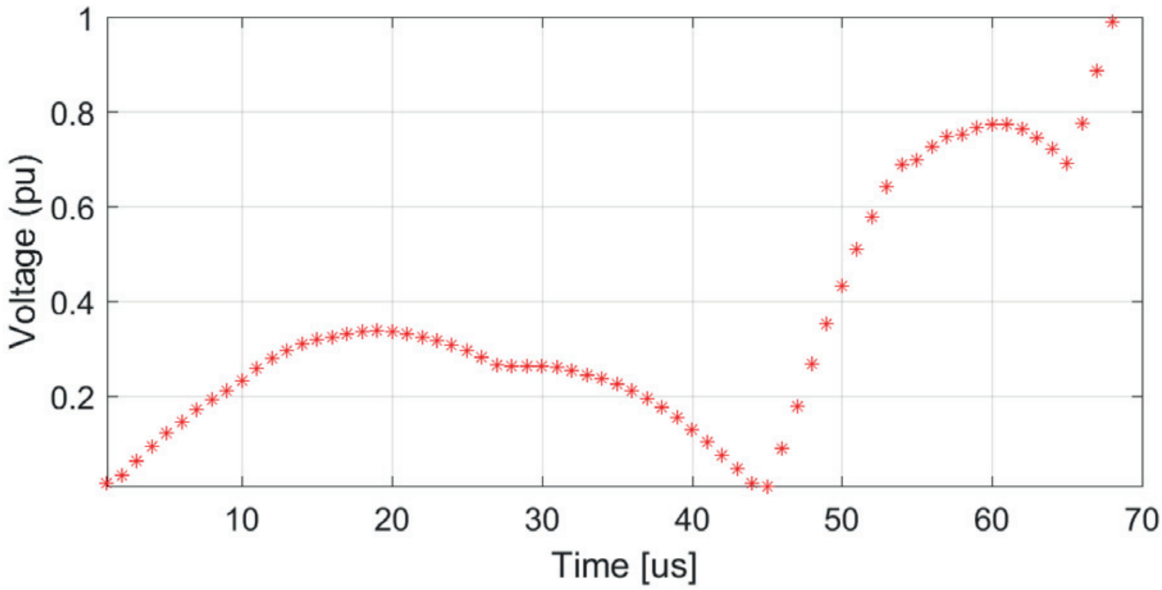

Figure 5: Maximum internal nodes voltages calculated with the Grey Box model

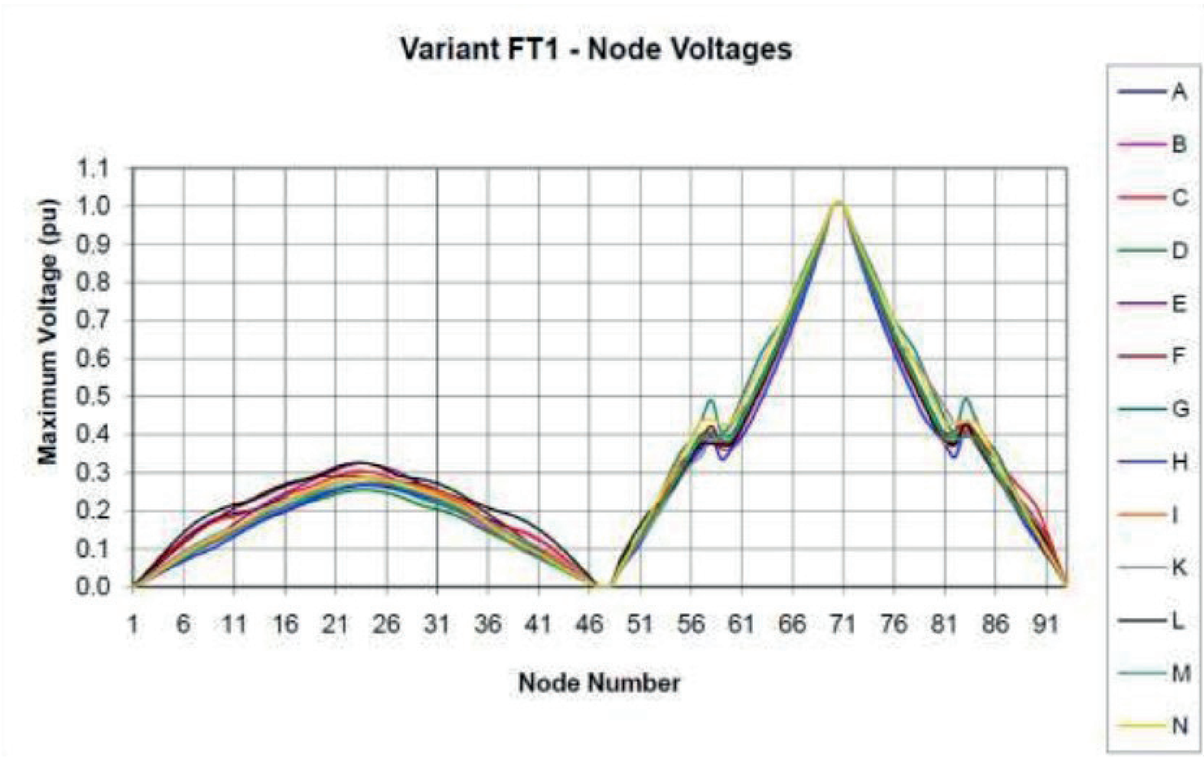

Figure 6: Maximum internal nodes voltages from CIGRE brochure [1]

In Figure 6 the results have been shown for 13 different transformer models developed by different universities, manufacturers or independent consultants. Note that the models used by CIGRE differs two parts of the HV winding. Consequently, the CIGRE results include voltages for more nodes. However, the numbers of the nodes correspond to each other in Figure 5 and Figure 6.

The presented model gave quite comparable results to the one provided by CIGRE especially if we take into account that the initial intention of the model was to study external voltages rather than the internal ones [3].

Furthermore, the comparison has been made for the voltage shapes existing at the first disc of the HV winding, seen from the point of the LI impact.

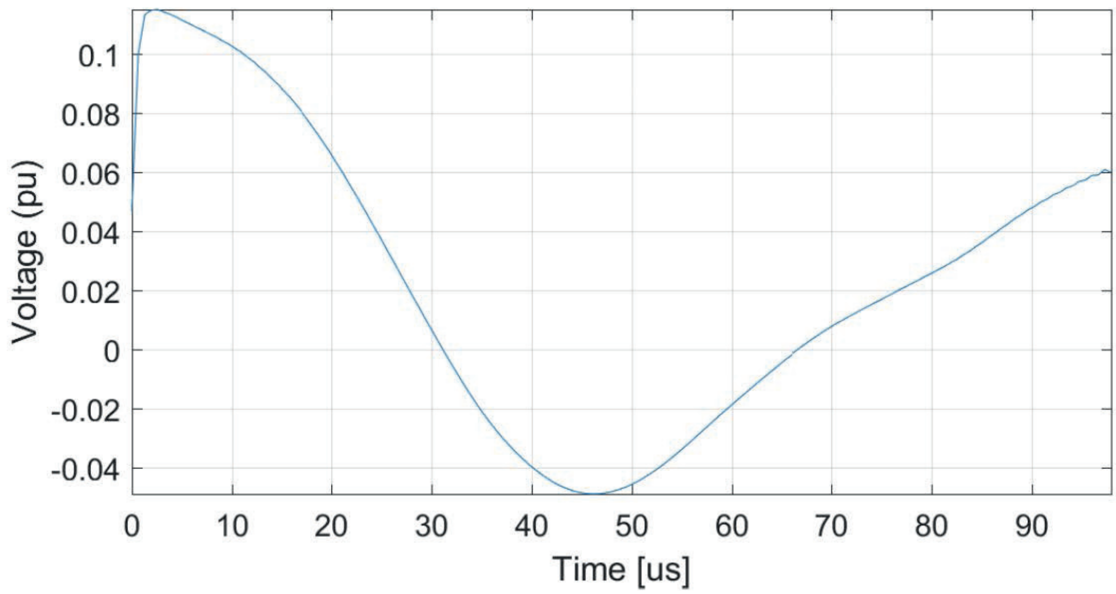

Figure 7: Voltage across the first discs of the HV winding calculated using the Grey Box model

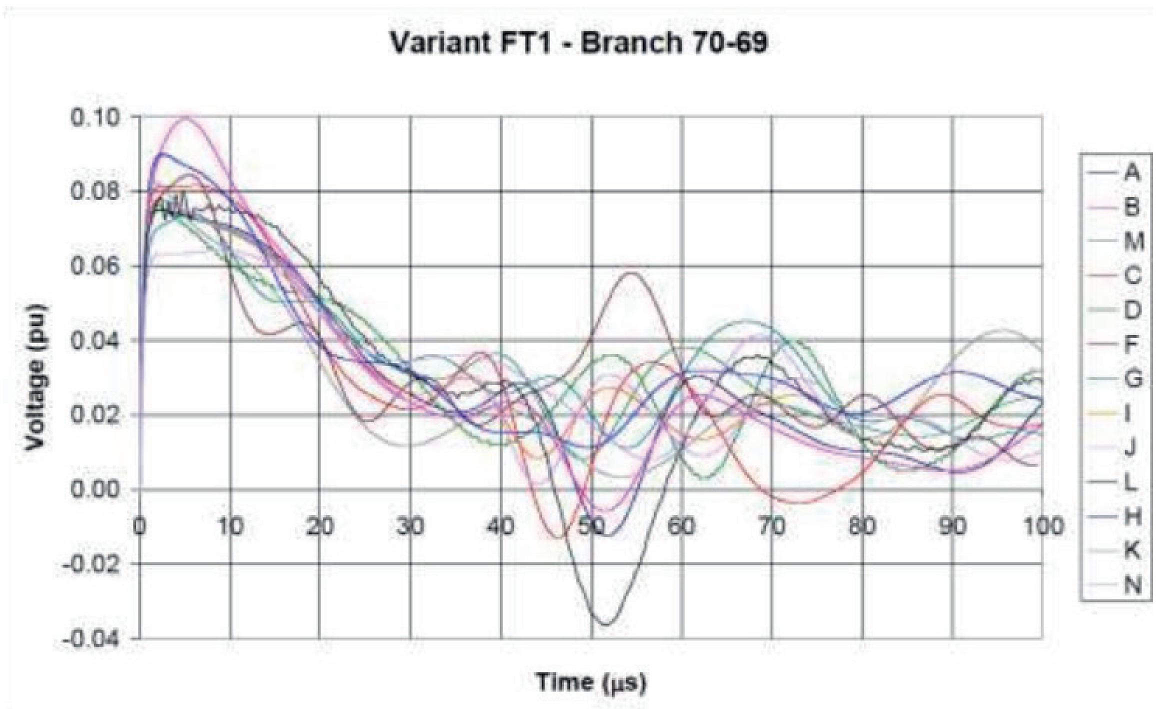

Figure 8: Voltage across the first discs of the HV winding from CIGRE brochure [1]

The model showed once again comparable results with the one provided by CIGRE.

Discrepancies between the results of the models could be explained by the validity range of the Grey Box model or due to the way parallel HV winding is presented.

5. CONCLUSIONS

In this paper a Grey Box model based on limited information about a transformer geometry has been presented. It has been validated, using the example from CIGRE brochure [1] for calculation of internal overvoltages along the transformer winding. It gave comparable results in terms of voltage amplitude and wave shapes, when compared to more advanced transformer models developed by different universities, manufacturers or independent consultants.

The models such as the one that is presented can help power utilities to detect the cause of transformer failure or to improve the design and protection of the power network.

6. REFERENCES

[1] CIGRE WG A2/C4.39, *Electrical Transient Interaction Between Transformers and the Power Systems*. 2013.

[2] S. V. Kulkarni and S. A. Khaparde, *Transformer Engineering Design and Practice*. 2004.

[3] B. Jurisic, "Methods for Calculations of High Frequency Transmitted Overvoltages through a Power Transformer," Ph.D. dissertation, University of Zagreb, University Blaise Pascal, 2016.

[4] B. Jurišić, P. Poujade, A. Xemard, I. Uglesic, and F. Paladian, "Calculation of internal overvoltages using a wide band transformer model based on limited information about transformer design," in *4th International Colloquium "Transformer Research and Asset Management,"* 2017, vol. 0, pp. 1–9.

[5] International Electrotechnical Commission, *IEC 60071-4 Insulation Co-ordination - Part 4: Computational Guide to Insulation Co-ordination and Modelling of Electrical Networks*. 2004.

[6] International Electrotechnical Commission, *IEC 60060-1 High-Voltage Test Techniques Part 1: General Definitions and Test Requirements*. 2010.

[7] J. a. Martinez-Velasco, *Power System Transients*. United States: CRC Press, 2010.

[8] E. Bjerkan, “High Frequency Modeling of Power Transformers,” Ph.D. dissertation, Norwegian University of Science and Technology, 2005.

[9] E. Bjerkan, H. K. Høidalen, and O. Moreau, “Importance of a Proper Iron Core Representation in High Frequency Power Transformer Models,” *IEEE Trans. Magn.*, vol. 34, no. 5, 1998.

[10] B. Jurisic, I. Uglesic, A. Xemard, and F. Paladian, “High frequency transformer model derived from limited information about the transformer geometry,” *Int. J. Electr. Power Energy Syst.*, vol. 94, pp. 300–310, 2018.

[11] M. David, “Finite Element Method Magnetics.” 2014.

[12] O. Moreau, L. Popiel, and J. L. Pages, “Proximity Losses Computation with a 2D Complex Permeability Modelling,” *IEEE Trans. Magn.*, vol. 34, no. 5, pp. 3612–3615, 1998.

[13] International Electrotechnical Commission, *IEC 60076-3- Power Transformers - Part 3: Insulation Levels, Dielectric Tests and External Clearances in Air*. 2013.